

Reflection and Reprocessing of X-ray Source Radiation by the Atmosphere of the Normal Star in a Binary System

M. M. Basko and R. A. Sunyaev

Institute of Applied Mathematics, Academy of Sciences of the USSR, Moscow, USSR

L. G. Titarchuk

Institute for Cosmic Research, Academy of Sciences of the USSR, Moscow, USSR

Received July 4, 1973

Summary. In a close binary system, up to 30% of the X-ray source radiation reaching the surface of the normal star is reflected. The remaining 70% is absorbed and is subsequently re-radiated as optical and ultra-violet radiation. In this paper, we consider the case of a semi-infinite plane atmosphere in a stream of hard X-rays, and we solve numerically the X-ray transfer equation. Photoabsorption and Compton scattering are taken into account. The albedo of the reflected X-rays is found; we have also obtained their spectral, polarizational, spatial and temporal (for a pulsation primary flux) characteristics.

The results obtained are discussed with specific reference to Her X 1, Cyg X3 and 2U 1700-37. We note that there may well exist X-ray sources which are weak

at about $h\nu \sim 2 \div 6$ keV, but bright at $h\nu \sim 15 \div 20$ keV; in the case of Her X1, there is an interval of 24 days (out of a total of 36) when the Earth is not in the beam of X-ray pulsar: the system is then visible only by virtue of the X-ray flux reflected by the surface of HZ Her, and it may then be such a source.

We note also that the transformation of soft X-rays in the atmosphere of HZ Her cannot account for its optical variability which, however, can be easily explained by the reprocessing hard X-rays. Two sources of the optical fluctuations of HZ Her = Her X1 are also discussed.

Key words: X-ray binary systems – radiative transfer – X-ray albedo.

I. Introduction

Many compact Galactic X-ray sources appear as parts of binary systems, a normal optical star being the second member (Tananbaum, 1972; Gursky, 1972). In a close binary system much of the X-ray source radiation reaches the surface of the optical star, and so the optical appearance of such a system is to a considerable extent determined by the way in which X-rays are converted into optical radiation by the atmosphere of the normal star (Shklovsky, 1967; Shakura and Sunyaev, 1973; Bahcall and Bahcall, 1972; Lyutiy *et al.*, 1973). Furthermore, the stellar surface may also shed some of its mass due to X-ray heating; both problems have recently stimulated considerable interest (Basko and Sunyaev, 1973; Pringle, 1973; Arons, 1973).

The X-rays are absorbed through the photoionization of hydrogen, helium and the K-electrons of heavy elements. This process is effective for low energy quanta but its cross-section rapidly decreases with increasing frequency: $\sigma_{\text{ph}}(\nu) \propto \nu^{-3}$. In a weakly ionized plasma with normal cosmic abundance, the Thomson scattering cross-section $\sigma_T = 6.65 \times 10^{-25} \text{ cm}^2$ has exceeded the

photoionization cross-section per hydrogen atom already when the photons have reached $h\nu_0 = 8 \text{ keV}$ (Bethe and Salpeter, 1957; Brown and Gould, 1970).

The ionization of hydrogen, which supplies a major fraction of the free electrons, has in practise little effect on both the photoabsorption cross-section (since it is mainly the heavy elements which are active in the photoabsorption of photons with $h\nu > 1 \text{ keV}$) and the scattering cross-section. At energies $h\nu > \alpha m_e c^2 \approx 3.7 \text{ keV}$ the photon wavelength is less than the Bohr radius, and the scattering of hard X-rays from hydrogen and helium atoms leads to a tearing off of a bound electron, since the recoil energy $\sim h\nu(h\nu/m_e c^2)$ is then much greater than the ionization potential of hydrogen: $\chi_H = \frac{1}{2}\alpha^2 m_e c^2$. Consequently the cross-section for scattering from electrons bound in hydrogen atoms is equal

to that from free electrons. Here, $\alpha = \frac{2\pi e^2}{hc} = 1/137$ is the fine structure constant.

However, the high degree of ionization of helium and heavy elements such as C, N, O, Ne decreases the photo-

absorption cross-section, and moves the point at which $\sigma_{\text{ph}}(\nu_0) \approx \sigma_T$ to lower photon energies, i.e. to below 8 keV.

Thus, the fate of X-ray quanta striking the photosphere of the normal star depends on their initial energy: at $h\nu \lesssim 8$ keV they are absorbed and transformed into soft (in particular optical) radiation; at $h\nu \gg 8$ keV a considerable fraction of the incident photons (17% after just the first scattering) is reflected (Basko and Sunyaev, 1973).

A number of compact X-ray sources (in particular both of the X-ray pulsars which are parts of the binary systems Her X 1 and Cen X 3) have anomalously hard X-ray spectra: $kT_x \sim 30$ keV (Ulmer *et al.*, 1972). Therefore, it is particularly interesting to find out how much of the incident energy is reflected- to obtain the albedo of the normal component in the hard X-ray region. On the one hand, we would like to know the efficiency with which X-rays are reprocessed in the atmosphere of the normal component of the binary system, and, on the other, the characteristics of the reflected signal have some intrinsic interest, especially during the interval when the beamed primary radiation does not scan across the Earth.

Note that the energy of hard X-rays is absorbed not only through photoionization (after which the photon "perishes"), but also as a consequence of recoil by scattering:

$$\Delta v/v \sim -h\nu/m_e c^2.$$

The recoil effect acts in two distinct ways: at every scatter, a part of the photon energy is transferred to the electron, and so after $\sim m_e c^2/h\nu$ scatter the photon loses a considerable part of its initial energy; moreover, the probability of photoabsorption, which increases with decreased photon energy, increases after each scatter, and so the albedo is decreased. In the case of energetic quanta, energy is absorbed mainly through the recoil effect. For example, the plane albedo of a monochromatic line $h\nu = 30$ keV is 47%. Numerical calculations in which the photoabsorption had been neglected ($\sigma_{\text{ph}} \equiv 0$) gave this albedo as 65% (see Table 1), i.e. the energy absorption had dropped by one third only.

In the third section of this paper, we present the values of plane and spherical albedo (see also Table 1). These were obtained from numerical solutions of the equation of X-ray transfer in a plane atmosphere (taking into account scattering and photoabsorption processes). The short time scale fluctuations of reflected X-rays (subsection IV, d) and the optical radiation arising from X-ray reprocessing (IV, e) are also discussed.

The fifth section is devoted to astrophysical applications. We have obtained what energy fraction of the X-ray flux of Her X 1 is transformed into the optical radiation of its visible companion. It is shown that soft X-rays (for which $h\nu < 1$ keV), which have been proposed by a number of authors (Avni *et al.*, 1973; Pringle,

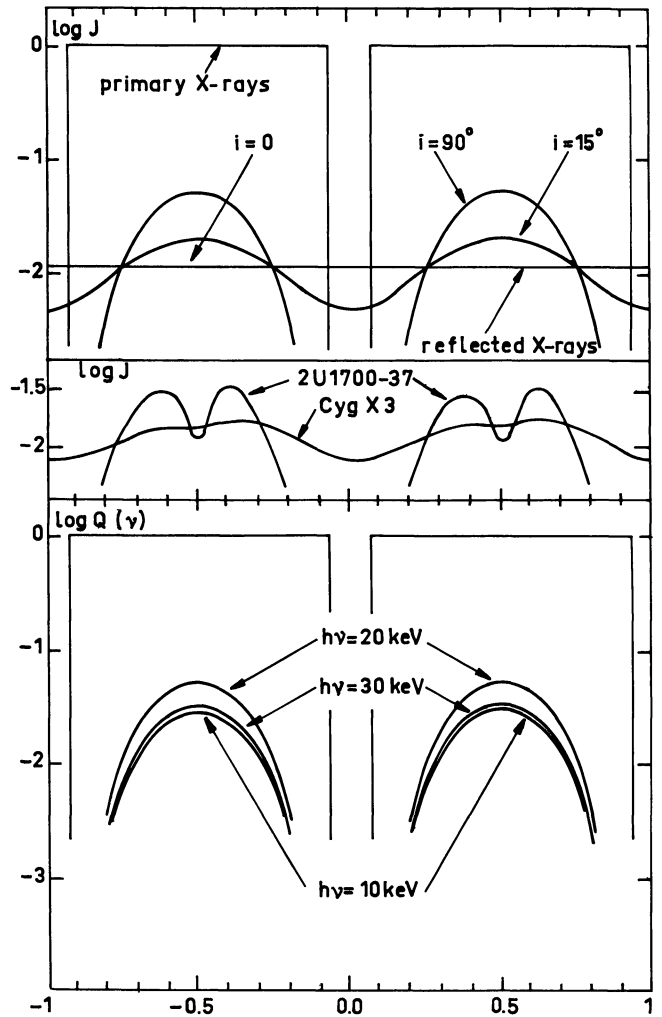


Fig. 1. In Fig. 1a the integrated light curves of the HZ Her system in reflected X-rays (for different values of orbital inclination i) are plotted versus orbital phase. At the bottom the averaged observed X-ray light curves of Cyg X3 for a 4.8-hour cycle (Parsignault *et al.*, 1972) and of 2U 1700-37 versus orbital phase (Jones *et al.*, 1973) are shown. Fig. 1b shows the spectral X-ray light curves calculated for HZ Her system when the temperature of the primary X-rays kT_x is 30 keV

1973) as being responsible for the optical variability of HZ Her, cannot satisfactorily explain the observations – it is in fact necessary to invoke the phenomenon of reprocessing of hard X-rays.

Up to 30% of the hard X-ray flux ($h\nu \sim 15 \div 30$ keV) striking the surface of HZ Her should be reflected. Therefore, hard X-rays (at a level $\sim 10\%$ of the maximum value) from the system Her X 1 = HZ Her should be observable during those 24 days out of 36 when the tightly beamed soft X-rays ($h\nu \lesssim 10$ keV) do not scan across the Earth (see V, A.). This phenomenon – the reflection of hard X-rays by the surface of a normal star – makes it possible to search for X-ray pulsars whose beams never cross the Earth.¹⁾ Fig. 1 shows the

¹⁾ Otherwise, the reflection effect merely slightly distorts the X-ray light curve.

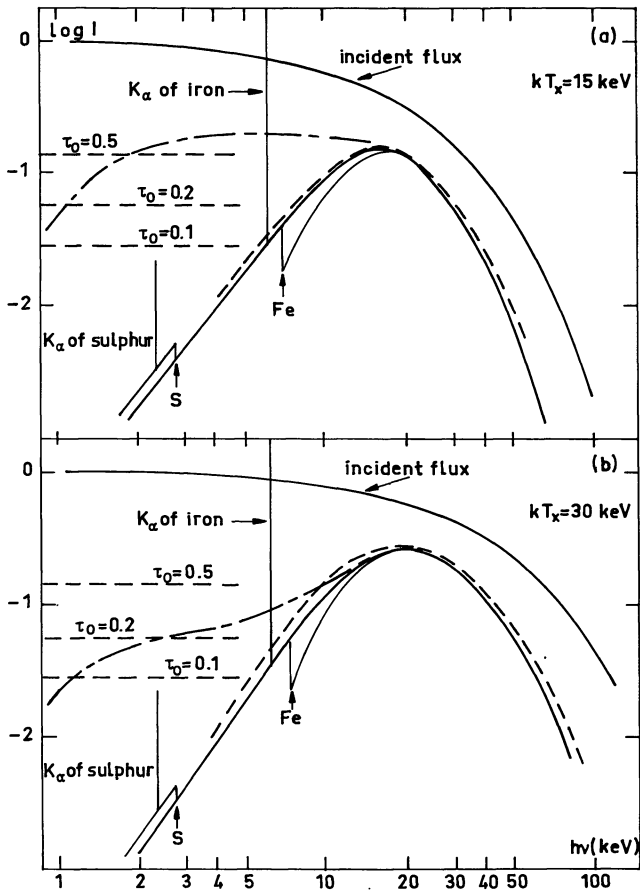


Fig. 2. The spectrum of X-rays reflected by a semi-infinite plane-parallel atmosphere. The primary flux has a spectral distribution of the form (11) with $kT_x = 15$ and 30 keV, and is perpendicular to the surface. Solid lines represent the spectrum of the flux reflected vertically and the dashed lines the spectrum reflected along the surface. The horizontal dashed lines correspond to the flux reflected by the external hot diffusive layer having a different optical depth for Thomson scattering τ_0 . The dashdot lines show the approximate form of the spectrum when such a layer is present. The normalization is explained in Section III. The fine structure of the spectrum is shown with a thin line

X-ray light curve of such systems. This curve is rather like the ones observed for Cyg X 3, when the orbital inclination $i \sim 10 \div 15^\circ$, and for 2 U 1700–37, when $i \sim 90^\circ$.

The spectrum of the reflected X-ray flux is shown in Fig. 2. It has a maximum at $h\nu \sim 15 \div 20$ keV. Consequently, there may very well be sources that radiate hard X-rays, but are practically unobservable in the usual band $h\nu \sim 2 \div 6$ keV. However, it is shown in subsection IV, b that under certain conditions the surface of the normal star itself may effectively reflect X-rays in the range $h\nu \sim 3 \div 10$ keV.

The spectrum of the reflected X-ray flux should contain jumps corresponding to the K-edges of photoabsorption by the heavy elements Fe, S and Ar. One of the most important features of the reflected signal is a strong emission in the K_α -line of iron. As a consequence

of Thomson scattering, the reflected signal should be quite highly polarized. The degree of polarization depends strongly on the inclination of the orbit.

II. Equations of X-ray Transfer in a Plane Atmosphere

a) Basic Assumptions

Hard X-rays with $h\nu \gtrsim 10$ keV striking the surface of a normal star are scattered and absorbed in the vicinity of photosphere in which $T_e \lesssim 2 \times 10^4$ K (Basko and Sunyaev, 1973). Consequently, we may:

1) treat all parts of the stellar atmosphere as plane-parallel since the height H of the exponential atmosphere is about $\frac{kT_e R^2}{m_p GM}$ which is much less than the radius of the star R ;

2) neglect the ionization of K-electrons in the atoms of heavy elements and use the calculations on photoabsorption cross-section made by (Bell and Kingston, 1967; Brown and Gould, 1970).

3) take the electrons which are involved in a Compton scattering as being at rest, since $kT_e \ll h\nu (h\nu/m_e c^2)$. In our case, the interesting X-ray band lies in the region $2 \text{ keV} \lesssim h\nu \lesssim 50 \text{ keV}$ and we may assume that $x = h\nu/m_e c^2 \ll 1$, the isotropic indicatrix and Thomson cross-section of scattering to be accurate enough approximations.

The basic equations on which the numerical calculations were based are given below.

Let us introduce a coordinate system OXYZ, which is such that the density decreases along the OZ-axis which is perpendicular to the stellar surface. The external radiative flux $H(\nu)$ [erg/cm² s Hz] strikes the atmosphere (the beam is in the OXZ plane) at an angle $\vartheta_0 = \arccos \mu_0$ with respect to OZ-axis. The optical depth with respect

to Thomson scattering $\left(\tau = \sigma_T \int_z^\infty N_e(z) dz\right)$, the azimuth angle φ measured from the OX-axis in the OXZ plane, and $\mu = \cos \vartheta$ (where ϑ is the polar angle measured from the OZ-axis) are used below as independent variables. We use the following form for the full absorption cross-section of X-rays of frequency ν :

$$\sigma(\nu) = \sigma_T + \sigma_{\text{ph}}(\nu) = \sigma_T [1 + (\nu_0/\nu)^3]$$

where $h\nu_0 = 8$ keV. Normal chemical abundances are assumed throughout. The albedo of a single scattering is given by:

$$\lambda(\nu) = \sigma_T/\sigma(\nu) = [1 + (\nu_0/\nu)^3]^{-1}.$$

b) The Equation of Transfer

The equation of X-ray transfer, when the scattering against electrons at rest is assumed to be isotropic, and when the recoil effect and photoabsorption are taken

into account, may be written as:

$$\begin{aligned} \mu \frac{\partial I(v, \tau, \mu, \varphi)}{\partial \tau} &= \lambda^{-1}(v) I(v, \tau, \mu, \varphi) \\ &- \frac{1}{4\pi} \int_0^{2\pi} d\varphi' \int_{-1}^{+1} \frac{v}{v'} \frac{\partial v'}{\partial v} I(v', \tau, \mu', \varphi') d\mu' \\ &- \frac{1}{4\pi} \frac{v}{v_1} \frac{\partial v_1}{\partial v} H(v_1) \exp[-\tau \mu_0^{-1} \lambda^{-1}(v_1)] \end{aligned} \quad (1)$$

where $I(v, \tau, \mu, \varphi)$ is the X-ray intensity,

$$v' = v/[1 - (hv/m_e c^2)(1 - \cos \gamma)] \quad (2)$$

$$\cos \gamma = \mu \mu' + \sqrt{(1 - \mu^2)(1 - \mu'^2)} \cos(\varphi - \varphi'),$$

$$v_1 = v/[1 - (hv/m_e c^2)(1 + \cos \gamma_0)] \quad (3)$$

$$\cos \gamma_0 = \mu \mu_0 + \sqrt{(1 - \mu^2)(1 - \mu_0^2)} \cos \varphi.$$

Note that (2) and (3) imply that: $\frac{\partial v'}{\partial v} = \left(\frac{v'}{v}\right)^2$ and $\frac{\partial v_1}{\partial v} = \left(\frac{v_1}{v}\right)^2$.

Writing the source function in the form:

$$\begin{aligned} S(v, \tau, \mu, \varphi) &= \frac{1}{4\pi} \int_0^{2\pi} d\varphi' \int_{-1}^{+1} \left(\frac{v'}{v}\right) I(v', \tau, \mu', \varphi') d\mu' \\ &+ \frac{1}{4\pi} \frac{v_1}{v} H(v_1) \exp[-\tau \mu_0^{-1} \lambda^{-1}(v_1)] \end{aligned}$$

and solving (1) with the boundary condition $I(v, \tau, \mu, \varphi) \Big|_{\mu < 0} = 0$, we obtain the following integral equation for S :

$$\begin{aligned} S(v, \tau, \mu, \varphi) &- \frac{1}{4\pi} \int_0^{2\pi} d\varphi' \left\{ - \int_{-1}^0 \frac{v'}{v} \frac{d\mu'}{\mu'} \int_0^\tau \right. \\ &\cdot \exp[(\tau - \xi) \mu'^{-1} \lambda^{-1}(v')] S(v', \xi, \mu', \varphi') d\xi \\ &+ \left. \int_0^1 \frac{v'}{v} \frac{d\mu'}{\mu'} \int_\tau^\infty \exp[(\tau - \xi) \mu'^{-1} \lambda^{-1}(v')] S(v', \xi, \mu', \varphi') d\xi \right\} \\ &= \frac{1}{4\pi} \frac{v_1}{v} H(v_1) \exp[-\tau \mu_0^{-1} \lambda^{-1}(v_1)]. \end{aligned} \quad (4)$$

c) The Approximations

In our frequency range we may assume that $x = \frac{hv}{m_e c^2} \ll 1$. From Eq. (4) we can see that $S(v, \tau, \mu, \varphi)$ depends on μ and φ only through v' and v_1 . If the variation of the right hand side of this equation in the spectral interval $\Delta v = v \frac{hv}{m_e c^2} = \frac{m_e c^2}{h} x^2$ (which in fact corresponds to the average frequency shift of the

photon after a single scattering) is negligible, i.e. if:

$$\frac{\Delta H}{H} = \frac{1}{H} \frac{\partial H}{\partial x} x^2 \ll 1 \quad (5)$$

then, since the solution of the integral Eq. (4) is a continuous function of its right hand side, the source function varies only slightly with μ and φ . Consequently, it is sufficiently accurate to simply average the source function over the angles φ and ϑ , obtaining thus the quantities $S_3(v, \tau, \mu) = \frac{1}{2\pi} \int_0^{2\pi} S(v, \tau, \mu, \varphi) d\varphi$ and $S_2(v, \tau) = \frac{1}{2} \int_{-1}^{+1} S_3(v, \tau, \mu) d\mu$. $S_3(v, \tau, \mu)$ is easily calculated to second order in x by substituting $v' = v/[1 - x(1 - \mu\mu')]$ and $v_1 = v/[1 - x(1 + \mu\mu_0)]$ in Eq. (4) (we call this Approximation III). $S_2(v, \tau)$ is found by substituting $v' = v_1 = v/(1 - x)$ (we call this Approximation II). It was Approximation II that was used in numerical calculations; the integral equation for S_2 may then be written as:

$$\begin{aligned} S_2(x, \tau) &= \frac{1}{1-x} \frac{1}{2} \int_0^\infty E_1 \left(|\tau - \xi|/\lambda \left(\frac{x}{1-x} \right) \right) \\ &\cdot S_2 \left(\frac{x}{1-x}, \xi \right) d\xi + \frac{1}{4\pi} \frac{1}{1-x} H \left(\frac{x}{1-x} \right) \\ &\cdot \exp \left[-\tau/\mu_0 \lambda \left(\frac{x}{1-x} \right) \right] \end{aligned} \quad (6)$$

where $E_n(x) = \int_1^\infty \exp(-\xi x) \xi^{-n} d\xi$ is an integral form of order n . Approximation I (the least accurate) differs from Approximation II in that the value of $S_2(x, \xi)$ at $\xi = \tau$ is factored out of the integrand in Eq. (6). Note that $E_1(x) = -\ln x + O(x)$ as $x \rightarrow 0$, and that $\int_0^\infty E_1(x) dx = 1$. Thus, in the limit of Approximation I:

$$\begin{aligned} S_1(x, \tau) &= \frac{1}{1-x} \lambda \left(\frac{x}{1-x} \right) \left[1 - \frac{1}{2} E_2 \left(\tau/\lambda \left(\frac{x}{1-x} \right) \right) \right] \\ &\cdot S_1 \left(\frac{x}{1-x}, \tau \right) \\ &+ \frac{1}{4\pi} \frac{1}{1-x} H \left(\frac{x}{1-x} \right) \exp \left[-\tau/\mu_0 \lambda \left(\frac{x}{1-x} \right) \right] \end{aligned} \quad (7)$$

Approximation III is not really a more accurate form than Approximation II as far as the angular dependence is concerned, since φ is as important a parameter as μ ; however, we may get some idea about the errors involved by comparing the two approximations.

The solid lines in Fig. 3 and 4 show the intensity of the reflected flux obtained by using Approximation II, the dotted lines are obtained from Approximation I, and the dashed line in Fig. 4 has been calculated from Approximation III. In Fig. 4 the spectra of incident and

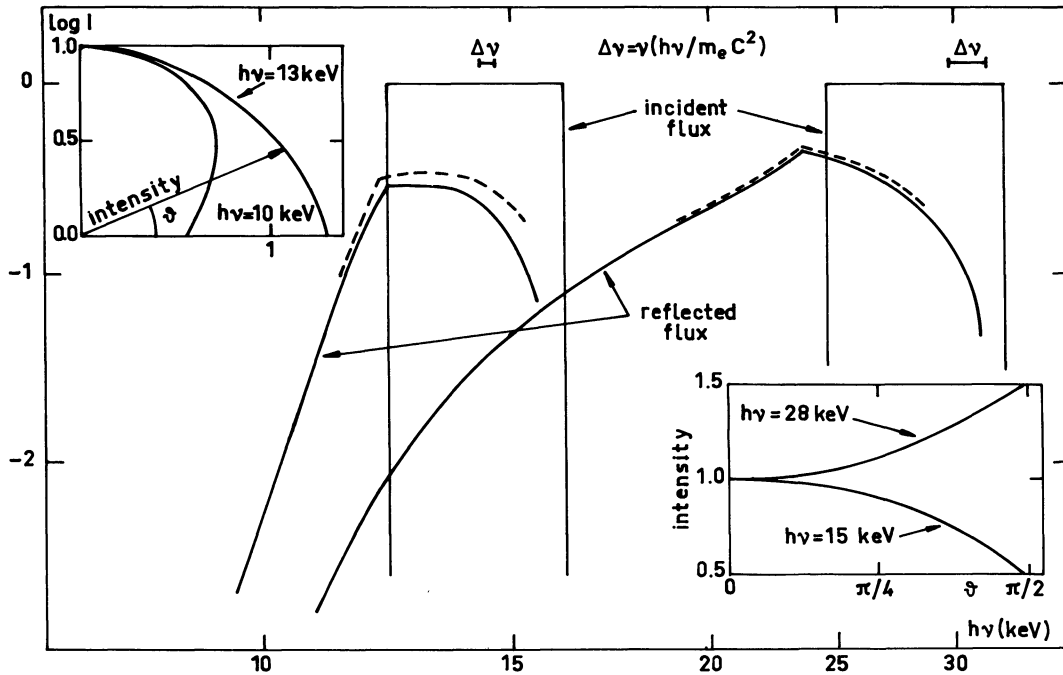


Fig. 3. The spectrum of the reflected flux when a monochromatic line with $h\nu=15$ and 30 keV strikes a plane atmosphere vertically. The plot in the upper left corner represents in polar coordinates a beaming of reflected X-rays for two values of the "exit" energy when the incident line has $h\nu=15$ keV. The same quantities are shown in the usual coordinate system in the lower right corner for an incident line with $h\nu=30$ keV

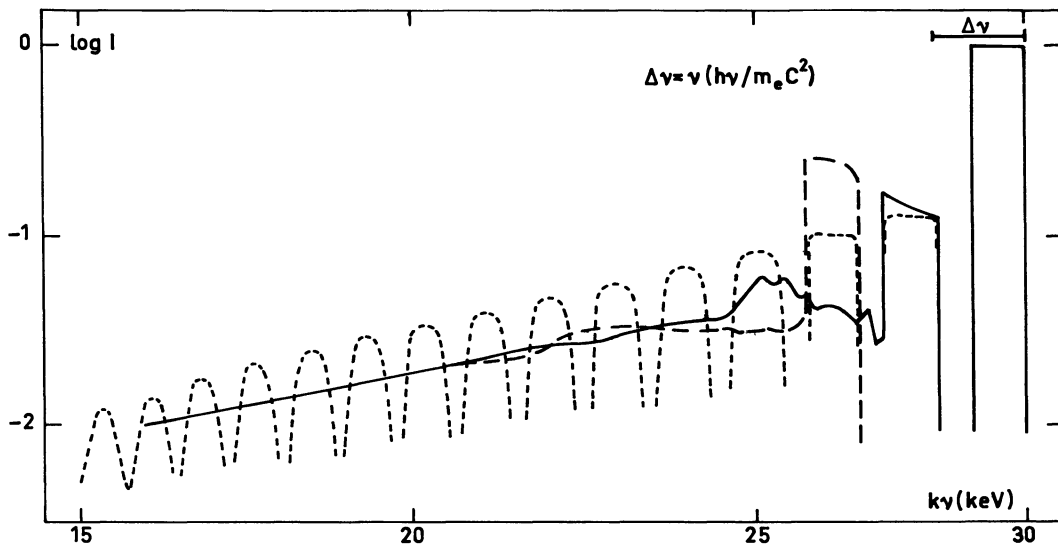


Fig. 4. The spectrum of the X-ray flux reflected along the normal to the plane atmosphere when the monochromatic line $h\nu=30$ keV falls normally on the surface. The dotted line represents the results of calculations according to Approximation I, the solid one-Approximation II, the dashed one-Approximation III (see Section II)

reflected X-ray fluxes are plotted for $\mu = \mu_0 = 1$, when an incident flux at $h\nu = 30$ keV is confined to a narrower spectral interval than $\Delta\nu = \nu x$. Condition (5) is then violated, and we note a significant difference between Approximations II and III, they may therefore not be used to determine the X-ray flux which emerges after a few scattering have taken place. Nevertheless, the albedo (an integrated quantity) is practically the same

in both approximations. The presence of a narrow peak in the reflected flux, shifted down in frequency by $2\Delta\nu$, is a natural consequence of the fact that X-ray photons must "turn about" before escaping from the atmosphere. In the case of the broad spectrum (11), condition (5) holds sufficiently accurately and the spectral differences between Approximations II and III do not exceed 3%: we are therefore quite justified in using Eq. (6). Note

that Eqs. (6) and (7) are not actually integral equations, but recurrence relations.

The plane energy albedo A_p , the photon number albedo A_{pn} and the mean number of times that the incident X-ray photons scatter before being absorbed or escaping from the atmosphere were calculated from the following expressions:

$$A_p = \frac{2\pi}{\mu_0} \frac{\int_0^\infty dx \int_{-1}^{+1} \mu I(x, o, \mu) d\mu}{\int_0^\infty H(x) dx}, \quad (8)$$

$$A_{pn} = \frac{2\pi}{\mu_0} \frac{\int_0^\infty x^{-1} dx \int_{-1}^{+1} \mu I(x, o, \mu) d\mu}{\int_0^\infty H(x) x^{-1} dx}, \quad (9)$$

$$\bar{N} = \frac{4\pi}{\mu_0} \frac{\int_0^\infty x^{-1} \lambda^{-1}(x) dx \int_0^\infty S_2(x, \tau) d\tau}{\int_0^\infty H(x) x^{-1} dx}. \quad (10)$$

The quantity \bar{N} is the ratio of a full number of scatters in a vertical column (of unit area) of the atmosphere, to the flux of incident photons.

d) The Plane Energy Albedo as a Function of the Incident Photon Energy

Consider a monochromatic beam of photons, crossing plane-parallel atmosphere in a vertical direction. Two extreme cases will be considered — they correspond to low and high frequencies.

1) The scattering is isotropic and monochromatic, there is significant photoabsorption but recoil by scattering is negligible: $\lambda(v) = [1 + (v_0/v)^3]^{-1}$, $v' = v$, $v'_1 = v$.

2) The photons are scattered against electrons at rest, photoabsorption is negligible, $\lambda(v) \equiv 1$, and the exact relativistic formulae are used to calculate the cross-section and the recoil energy distribution.

Case 1) is a good model for the reflection of soft X-rays $h\nu \ll 8$ keV by an atmosphere having a normal chemical composition. It has already been analysed in detail (Ivanov, 1969; Sobolev, 1972), and the corresponding value of plane albedo $A_{p1}(x)$ is plotted in Fig. 5 as a function of frequency ($x = h\nu/m_e c^2$).

Case 2) corresponds to the reflection of hard X- and soft γ -rays ($h\nu \gg 8$ keV). The approximate form of the plane albedo $A_{p2}(x)$ in this case is also shown in Fig. 5. Clearly, the real value of the albedo for a monochromatic line $A_p(x)$ should satisfy the conditions $A_p(x) < A_{p1}(x)$ and $A_p(x) < A_{p2}(x)$ (see Fig. 5). This implies that $A_p(x)$ has a maximum $A_p^* = A_p(x^*) < 1$ at some frequency x^* . Numerical calculations (see Table 1) and the estimates given below suggest that $h\nu^* = x^* m_e c^2 \approx 50$ keV and $A_p^* \approx 50\%$.

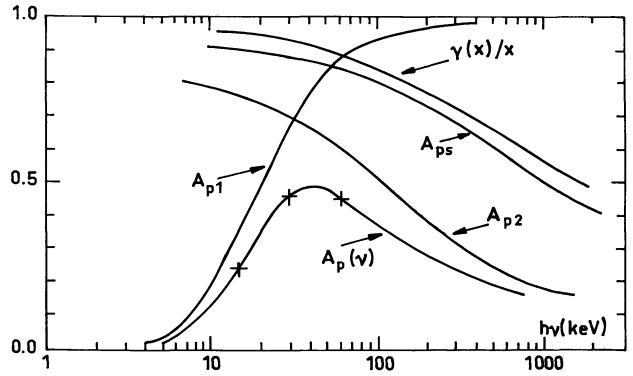


Fig. 5. The energy albedo of the plane semi-infinite atmosphere as a function of the energy of the vertically incident X-ray quanta: $A_p(v)$ -photoabsorption and recoil effect have been taken into account; $A_{p1}(v)$ -photoabsorption only; $A_{p2}(v)$ -the recoil effect only (qualitative behaviour); $A_{ps}(v)$ -an upper estimate for $A_{p2}(v)$ (see Subsection II, d); $\gamma(x)$ -the mean energy of photons (in $m_e c^2$ units) after they have scattered with an incident energy $x m_e c^2$; crosses correspond to calculated values of albedo

Let us now evaluate $A_{p2}(x)$. The differential cross-section for photons scattering from electrons at rest may be written in the form (Achiezer and Berestetski, 1969) $d\sigma(x, \zeta) = \frac{1}{2} \frac{e^4}{m_e^2 c^4} f(x, \zeta) d\Omega$, where $\arccos \zeta$ is the angle of scattering and where

$$f(x, \zeta) = \frac{1}{[1 + x(1 - \zeta)]^2} \left[1 + \zeta^2 + \frac{x^2(1 - \zeta)^2}{1 + x(1 - \zeta)} \right].$$

The mean energy (in units of $m_e c^2$) of photons after the first scattering is

$$\gamma(x) = \frac{\int_{-1}^{+1} x[1 + x(1 - \zeta)]^{-1} f(x, \zeta) d\zeta}{\int_{-1}^{+1} f(x, \zeta) d\zeta} = \frac{\omega(x)}{2\psi(x)};$$

$$\psi(x) = \frac{1}{2} \int_{-1}^{+1} f(x, \zeta) d\zeta = \left(\frac{1}{2x} - \frac{1+x}{x^3} \right) \ln(1+2x) + \frac{2}{x^2} + \frac{1+x}{(1+2x)^2},$$

$$\omega(x) = \frac{1}{x^2} \ln(1+2x) + \frac{1}{3} \left[1 - \frac{1}{(1+2x)^3} \right] + \frac{2x - 2 - 2/x}{1+2x}.$$

Since photons always lose energy when they scatter:

$$A_{p2}(x) < \gamma(x)/x = \frac{4}{3} (\ln x)^{-1} + O\left(\frac{1}{x}\right).$$

Consequently, $A_{p2}(x) \rightarrow 0$ as $x \rightarrow \infty$ and has the frequency dependence shown in Fig. 5. A better estimate for $A_{p2}(x)$ can be found by taking into account the frequen-

cy shift due to a second scattering

$$A_{p2}(x) < A_{ps}(x) = \frac{\varphi(x)}{2\psi(x)} \left[\frac{1}{1+x} - \frac{1}{x} \gamma \left(\frac{x}{1+2x} \right) \right] + \frac{\omega(\gamma(x))}{2\psi(x)},$$

where

$$\varphi(x) = \frac{2}{x^2} + \left(2 + \frac{1}{x} - \frac{3}{x^2} - \frac{2}{x^3} \right) \ln \frac{1+2x}{1+x} + \frac{2x^3 + \frac{9}{2}x^2 + \frac{7}{2}x + 1}{(1+2x)^2(1+x)^2} - 2 \ln 2.$$

The function $A_{ps}(x)$ is also shown in Fig. 5.

III. Results of Numerical Calculations

a) Reflection by a Plane Atmosphere

The results of numerical calculations are shown in Table 1 and in the figures. Figure 3 shows the intensity of a beam falling at an angle $\vartheta_0 = \arccos \mu_0 = 0$ and reflected by a plane semi-infinite atmosphere at an angle $\vartheta = \arccos \mu = 0$. The incident flux is confined to narrow spectral intervals near $h\nu_1 = 15$ keV and $h\nu_2 = 30$ keV. Note that the minimum width of these intervals is determined by the range within which the approximation used are still valid, i.e. condition (5).

The equation of X-ray transfer is linear in intensity $I(\nu)$ and initial flux $H(\nu)$ [erg/cm² s Hz]. The X-ray intensity is normalized in such a way that the spectral energy flux $\mu_0 H(\nu) = \pi$ falls upon unit surface area. Had the surface of the semi-infinite atmosphere reflected all this flux isotropically and without frequency shift, the reflected X-rays would have had unit intensity. The fraction of the reflected energy (the plane energy albedo), the fraction of the reflected photons and the mean numbers of scatters for incident X-rays with $h\nu = 15, 30$ and 60 keV are given in Table 1. With increasing photon

energy the accuracy of the non-relativistic approximation drops, and the real values of albedo for $h\nu = 60$ keV may be slightly different from those given in Table 1.

With increasing frequency photoabsorption becomes less important, but Compton energy losses caused by the recoil mechanism increase. Consequently, as the frequency of the incident flux ν increases, the monochromatic albedo $A_p(\nu)$ also increases for as long as $\nu < \nu^*$, reaches its peak value $A_p^* \sim 0.5$ at $h\nu^* \sim 50$ keV and then drops to zero as $\nu (> \nu^*) \rightarrow \infty$ (see Fig. 5 and II, d). Through this mechanism alone, therefore, more than half of the energy of the X-rays falling normally on the surface of the optical star is absorbed and goes to heat the atmosphere.

The diagram in the upper left hand corner of Fig. 3 shows the variation of the intensity of X-rays, plotted along the radius-vector, as a function of the polar angle ϑ at which photons leave the surface. Two values of energy for an incident monochromatic flux with $h\nu = 15$ keV are shown. In the lower right hand corner these are plotted for $h\nu = 30$ keV, with values of ϑ being the abscissae and the intensity values being the ordinates. We recall that a surface element of area dS reflects per unit solid angle the energy flux $dF_\nu(\vartheta) = I_\nu(\vartheta) \cos \vartheta dS$. Hard X-ray photons, which suffer one or two scatters only, emerge mainly at angles close to $\pi/2$, while soft photons, which are scattered many times, leave the surface in directions close to the normal.

Figure 2 shows the reflected spectrum when the normally ($\vartheta_0 = 0$) incident X-ray beam has a spectral shape given by:

$$H(\nu) = \pi \exp(-h\nu/kT_x). \quad (11)$$

Curves are plotted for $kT_x = 15$ and 30 keV. The solid line represents the spectrum of the emergent radiation at an angle $\vartheta = 0$, while the dashed line corresponds to the angle $\vartheta = \pi/2$. Corresponding values of the plane albedo are given in the lower part of Table 1.

Table 1

Monochromatic line $h\nu$ (keV)	The plane energy albedo A_p		The plane photon number albedo A_{pn}		The plane energy albedo A_p for $\sigma_{ph} \equiv 0$ $\mu_0 = 1$	The spherical energy albedo	The mean number of scatters \bar{N} $\mu_0 = 1$
	$\mu_0 = 1$	$\mu_0 = 0.5$	$\mu_0 = 1$	$\mu_0 = 0.5$			
15	0.24	0.33	0.27	0.36	0.75	—	6.7
30	0.47	0.6	0.6	0.73	0.65	—	30
60	0.45	0.6	0.7	0.8	0.5	—	45
Continuous spectrum with kT_x (keV)							
15	0.21	0.28	—	—	0.73	0.24	—
30	0.3	0.39	—	—	0.66	0.36	—

b) Reflection of X-rays by the Surface of the Normal Component of a Binary System

For numerical calculations the normal star was taken to be a sphere of radius $R = 0.42 A$, where $A = 6 \times 10^{11}$ cm is the distance between the two components; these parameters are the results of an analysis of observational data for the HZ Her system (Lyutiy *et al.*, 1973; Forman *et al.*, 1972; Basko and Sunyaev, 1973). The X-rays were assumed to be from a point source and to have a line shape of the form $F_x(\nu) \propto \exp(-h\nu/kT_x)$; we suppose that they fall on as much of the surface of the companion as is visible from the point source.

Reflected X-ray light curves of the system HZ Her = Her X1 (the radiative flux as a function of the orbital phase $0 \leq \zeta \leq 1$, where $\zeta = 0$ corresponds to the middle of the X-ray eclipse) are plotted both in Fig. 1b (which shows spectral curves $Q(\nu)$ for $h\nu = 10, 20$ and 30 keV), and in the upper part of Fig. 1a (which shows an integrated curve $J = \int Q(\nu) d\nu$). The X-ray temperature kT_x of Her X1 was taken to be 30 keV. The X-ray flux from HZ Her integrated over the entire spectrum is normalized to unit integrated-primary flux from Her X1, and the spectral flux is normalised to unit spectral flux from Her X1 at $h\nu \ll kT_x$. The brightness of the system in reflected X-rays is the flux of radiation per unit solid angle reflected to the observer from the whole visible area of the normal star. The top of Fig. 1a shows the integrated X-ray light curves of HZ Her for three values of the inclination angle ($i = 0^\circ$, $i = 90^\circ$, and $i = 15^\circ$), while the bottom shows the X-ray light curves of Cyg X3 and 2U 1700-37.

We can find the flux of reflected X-rays at the Earth by dividing the values shown in the figures by the square of the source distance r ; allowing for the normalization this gives:

$$f_x(\nu) = Q(\nu, \zeta, i) \frac{h}{kT_x} \frac{L_x}{4\pi r^2} [\text{erg/cm}^2 \text{ s Hz}]$$

$$j_x = \int_0^\infty f_x(\nu) d\nu = I(\zeta, i) \frac{L_x}{4\pi r^2} [\text{erg/cm}^2 \text{ s}].$$

The functions $Q(\nu, \zeta, i)$ and $I(\zeta, i)$ depend on the parameters of the system only through the ratio R/A (in the limit $R/A \ll 1$ they are proportional to $(R/A)^2$).

When the normal star fills its critical Roche lobe the ratio R/A is slightly related to the ratio of the masses of the two components M_x/M_y .

The spectrum of the reflected X-ray flux is to all intents and purposes that plotted in Fig. 2. The intensity reaches a maximum at $h\nu \sim 20$ keV.

Figure 1 shows that the reflected X-rays are cut off by the eclipse for rather long periods of time (approximately three times longer than the X-rays of Her X1). The X-ray light curves with $kT_x = 15$ keV are very similar to those with $kT_x = 30$ keV.

IV. Characteristics of the Reflected X-rays

a) Spectral Features of the Reflected Signal

At low frequencies $\nu \lesssim \nu_0$ ($h\nu_0 = 8$ keV is the energy of the photons where $\sigma_{\text{ph}}(\nu) = \sigma_T$), an overwhelming fraction of reflected photons have been scattered only once and the form of the spectrum of the reflected flux is completely determined by the way in which the photoabsorption cross-section varies with frequency. This implies that the reflected spectrum should contain jumps corresponding to the K-edges of photoabsorption on the most abundant of the heavy elements, (such as O, Ne, S and Fe). The mean spectral index α at low frequencies $\nu \ll \nu_0$ is equal to 3, and so an incident spectrum of the form (11) is usually reflected in the form of the Wien distribution.

Figure 2 shows the calculated spectrum, and the jumps corresponding to iron and sulphur are drawn with a thin line. The most interesting is the iron jump at $h\nu = 7.2$ keV, for at this energy the reflected flux has a rather large amplitude. The jump magnitude was estimated using a value of the absorption cross-section near the K-edge equal to $\sigma_{\text{Fe}} = 4.6 \times 10^{-20} \text{ cm}^2$ and an iron abundance $[\text{Fe}]/[\text{H}] = 4 \times 10^{-5}$. Now, the K-fluorescence yield ω_k is proportional to Z^4 and is negligible for atoms with a relatively small nuclear charge Z (carbon, oxygen, neon etc.), and so one does not expect to observe large numbers of K_α -lines for the heavy elements. The most likely candidate is the K_α -line of low ionized iron at $h\nu = 6.6$ keV. For iron, $\omega_k = 0.3$ (Fink *et al.*, 1966). Consequently, 30% of the hard X-ray photons which are absorbed by photoionization of iron are transformed into K_α -photons, and about half of these are not absorbed by the photosphere. The natural width of this line is small $-h\Delta\nu \approx 10$ eV – but scattering processes should spread it to lower frequencies. The amount of energy in the K_α -line of iron, and the magnitude of the jump in the photoabsorption cross-section, depend on the abundance of iron in the stellar atmosphere. Using the abundance quoted above, the K_α -emission of iron

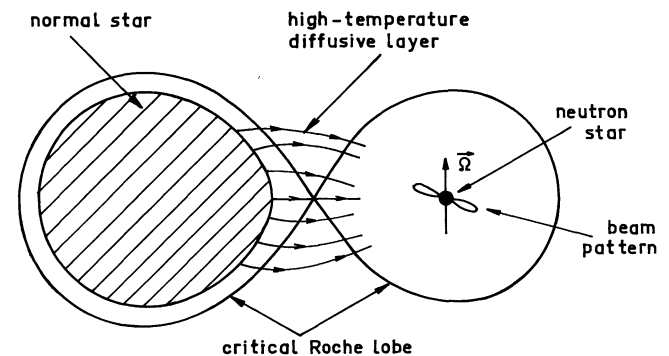


Fig. 6. A binary system containing X-ray pulsar and a highly ionized diffusive layer created by the matter evaporating from the normal star

turns out to be so strong that in the narrow spectral range $h\Delta\nu \lesssim 100$ eV ($\Delta\nu/\nu \sim 1/60$), its intensity exceeds that of the primary X-ray flux (the geometry of the binary system has been taken into account in the calculations). Therefore, this X-ray line is detectable for bright X-ray sources contained in close binaries, and its intensity may be a measure of the iron abundance. The discovery of the K_α -line of iron in Sco X1 could provide an extra argument in favour of its binary nature which has been discussed recently (Shklovsky, 1973; Basko and Sunyaev, 1973). Note that the intensity of the K_α -line depends on the inclination of the orbit i .

b) The High-Temperature Diffusive Layer Above the Stellar Surface and Its Contribution to the X-ray Reflectivity

The interaction of X-rays with the atmosphere of a normal-star gives rise to what is in effect a kind of evaporation, and matter is induced to leave its surface (Basko and Sunyaev, 1973; Arons, 1973) (see Fig. 6), i.e. produces an extra stellar wind. The outflowing gas is heated by the hard X-rays to high temperatures. The high degree of ionization of the heavy elements responsible for the photoelectric absorption of X-ray photons makes that contribution small relative to Compton scattering. The optical depth (with respect to Thomson scattering) of this high-temperature diffusive layer which lies above the stellar surface may reach quite significant values: $0 < \tau_0 \lesssim 1$. Numerical calculations (Basko and Sunyaev, 1973) have shown that $\tau_0 \approx 0.05$ in the particular case of the HZ Her = Her X 1 system (in other systems the optical depth may be much thicker). Elements such as oxygen, carbon, helium and hydrogen are completely ionized in this layer. The ratio of the abundance of O VIII to that of O IX is only $10^{-2} \div 10^{-3}$. The optical depth of this high-temperature zone with respect to photoabsorption turns out to be small for all photons with $h\nu \gtrsim 2$ keV. This layer makes a considerable contribution to reflection of X-rays in the range $h\nu \sim 2 \div 6$ keV.

The influence of the external layer, in which only pure scattering takes place since the recoil effect is negligible at $h\nu \lesssim 8$ keV, may readily be estimated by a method due to Sobolev (1972): he calculated the amount of difusive light reflected by a planetary atmosphere of finite optical depth τ_0 when surface albedo is known. Taking this latter quantity to be zero, the plane and spherical albedo may be derived with sufficient accuracy from the following approximate expressions:

$$A_p = \frac{3\tau_0 - (1 - e^{-\tau_0})}{4 + 3\tau_0}; \quad A_{\text{sph}} = \frac{\tau_0}{\tau_0 + 4/3}.$$

Therefore, the reflected X-ray spectrum in the range $2 \div 20$ keV may be quite flat: it will have the form shown in Fig. 2 with a dashdot line. The horizontal broken lines in this figure show the reflected X-ray intensity in the limit $h\nu \ll kT_x$. The characteristic frequency value ν_0 at which $\sigma_{\text{ph}}(\nu_0) \tau_0 / \sigma_T \sim 1$ and the flat spectrum is cut off (the low-frequency bound of the spectrum) depends on the degree of ionization of the heavy elements. This bound may vary with the primary X-ray flux or with the accretion rate.

c) The Polarization of Reflected X-rays

Thomson scattering on electrons will induce linear polarisation in initially unpolarised radiation: the degree of polarisation \mathcal{P} is given by $1 - \cos^2 \gamma$, where γ is the angle of scattering. Therefore the X-ray radiation reflected by the normal star should be linearly polarized except when the orbital phase is $\zeta = 0.5$. Photons of $h\nu \ll 8$ keV are scattered once only, and so their degree of polarization may easily be estimated—results for the plane atmosphere are given in (Sobolev, 1972). Since the reflecting surface is symmetrical there is no polarization when the phase $\zeta = 0.5$. As the orbital phase ζ changes, the degree of polarization of the reflected X-rays rapidly increases and reaches its peak value $\mathcal{P}_{\text{max}} \sim 60 \div 80\%$ in the phases $\zeta_1 \sim 0.25$ and $\zeta_2 \sim 0.75$.

When $h\nu \gtrsim 8$ keV, the reflected radiation is less polarized, since much of it suffers more than just a single scattering. If X-rays are initially polarised, the degree and type of polarisation changes after reflection. If only the first scatter is of importance, this effect can easily be estimated in every particular case.

The polarisation of an unpolarised X-ray beam, and its variation with orbital phase, may help us to distinguish between the reflected and the primary signals.

d) Short Time-Scale Pulsations of Reflected X-rays

In binary systems such as the X-ray sources Her X1 and Cen X3 the surface of the normal star is exposed to a pulsating X-ray flux, whose period p is of the order of a few seconds. After reflection the pulses should be blurred.

Let us assume that the normal star is a sphere of radius R , and is at a distance A from its companion. The amplitude of the reflected pulses will depend on two factors:

- 1) the finite time t_d that the X-ray photons “wander” in the atmosphere of the normal component;
- 2) the finite dimensions of the reflecting surface: these are comparable to cp , and so the signal reflected by different parts of the surface reaches the observer at different phases of the pulse.

Let us estimate the time t_d . The density distribution in the stellar atmosphere may be approximated

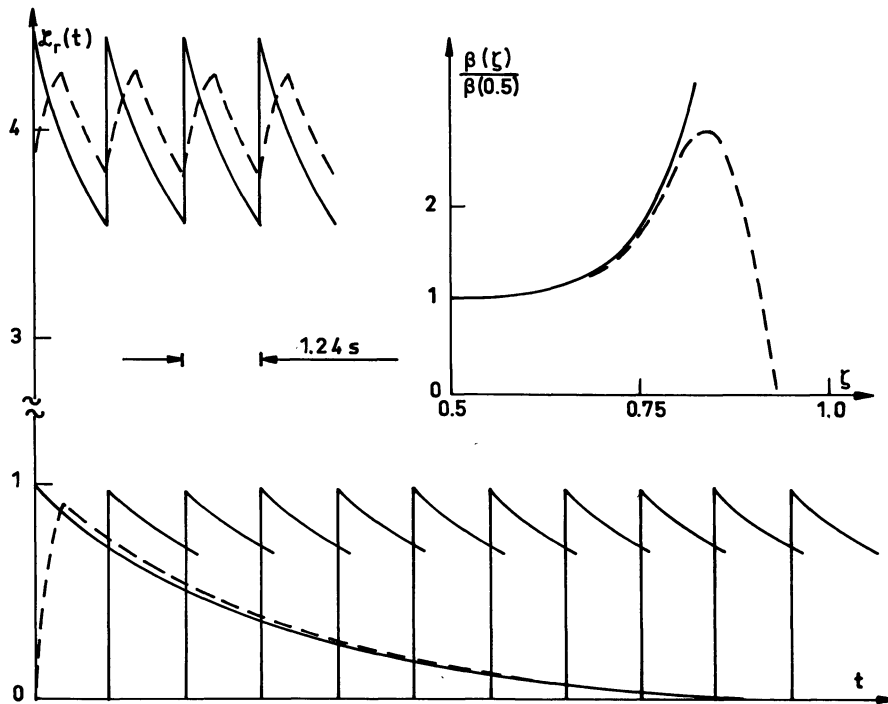


Fig. 7. Fluctuations of the reflected X-ray flux in the HZ Her system. At the bottom the luminosity of an individual ring strip is shown (IV, d), at the top – the summed flux of all strips. The solid line corresponds to infinitely narrow primary pulses (12), the dashed one – to rectangular pulses of duration $\Delta p = p/3$. Pulses of this latter kind should be observed in the case of a knife beam pattern. The upper right corner shows the pulse amplitude of reflected X-rays (solid line) and optical radiation (dashed line) as functions of the phase

with sufficient accuracy by the exponential form $N_e(z) = N_{e0} \exp(-z/H)$, where $H \approx \frac{kTR^2}{m_p GM}$ is the height of the homogeneous atmosphere. In the atmosphere of HZ Her this height comes to $10^8 \div 10^9$ cm. Introducing the optical depth with respect to Thomson scattering $\tau = \sigma_T \int_0^\infty N_e(z) dz$, we find that $N_e(\tau) = \tau / \sigma_T H$.

The mean number of scatters per emergent photon $\bar{N}_1(\nu)$ is considerably less than the $\bar{N}(\nu)$ which is given in Table 1 (calculated per incident photon). We recall that 17% of the incident photons emerge after one scatter only; photons which scatter many times penetrate to a considerable optical depth, lose energy through recoil and most of them are absorbed. The time during which the emergent photons have “wandered” can be estimated to be $t_d < \frac{\bar{N}_1(\nu)}{\sigma_T N_e(\bar{\tau}) c} \approx \frac{\bar{N}_1(\nu) H}{\bar{\tau} c}$.

Here $\bar{\tau} \geq 1$ is the optical depth of the layer where most scattering takes place. The most likely $\bar{\tau}$ is only a few times less than $N_1(\nu)$, and $t_d < 10 \frac{H}{c} \approx 0.03 \div 0.3 \text{ s} \ll 1.24 \text{ s}$. Thus the time for which photons are delayed in the atmosphere of the normal star is small, and so the amplitude of the X-ray pulses in the reflected flux is determined rather by the finite dimensions of the reflecting surface.

It is not very difficult to estimate the amplitude of the reflected X-ray pulses when the primary flux is radiated isotropically by a point source, and has a very narrow time spread:

$$L_x(t) = 4\pi \mathcal{L}_x(t) = 4\pi \langle \mathcal{L}_x \rangle p \sum_{k=-\infty}^{k=+\infty} \delta(t - kp) \quad (12)$$

Here p is the period, and $\langle \mathcal{L}_x \rangle$ is the X-ray luminosity of the primary per unit solid angle averaged over one period.

Consider the most simple case, when the inclination of the orbit i is 90° and the phase of observation ζ is 0.5, i.e. when the X-ray flux is at its maximum. When the primary pulses are infinitely thin, the observer will see a number of bright concentric rings running along the stellar surface. These rings rapidly become fainter as they move away from that point on the surface which is closest to the source, and their intensity is easy to estimate (see Fig. 7). New rings appear suddenly, and then slowly fade; the reflected signal will therefore be variable in time, and will have a slowly varying background due to the summed emission of the other rings ($[A\sqrt{A^2 - R^2} - (A - R)^2]/cpA \approx 9.5$ in the case of the HZ Her system).

If we take the photon delay time t_d to be 0: we can readily obtain the amplitude of the reflected flux per unit solid angle which is equal to the brightness of

appearing new ring:

$$\mathcal{L}_{ra} = 2\varrho(1,1) \frac{\langle \mathcal{L}_x \rangle}{A} \frac{R^2}{(A-R)(2A-R)}$$

where

$$A = R/cp, \quad \varrho(\mu, \mu_0) = \int_0^\infty I(v, \tau, \mu, \mu_0) dv \Big|_{\tau=0}$$

is the coefficient of reflection of the plane atmosphere when an incident beam of intensity $\pi\mu_0$ and direction $\arccos\mu_0$ is reflected at an angle $\arccos\mu$. The intensity $I(v, \tau, \mu, \mu_0)$ is defined in Section III and $I(v, 0, 1, 1)$ is shown in Fig. 2.

The mean value of the reflected X-ray flux (a time averaged sum of all rings) per unit solid angle is given by:

$$\mathcal{L}_r = 2\langle \mathcal{L}_x \rangle \int_{R/A}^1 \varrho(\mu, \eta) \frac{\eta \mu d\mu}{(A/R)^2 + 1 - 2A\mu/R},$$

where

$$\eta = (A\mu - R)/\sqrt{A^2 + R^2 - 2AR\mu}.$$

The relative amplitude $\beta(0.5) = \mathcal{L}_{ra}/\mathcal{L}_r$ is inversely proportional to $A = R/cp$. In the HZ Her system $A = 6.7$ and $\beta(0.5)$ is then about 0.3. The pulse amplitude of the reflected flux is smallest when the phase $\zeta = 0.5$, and so in other phases $\beta(\zeta) > 0.3$. β depends also on the shape of the primary pulse, decreasing when the pulse width increases. Arbitrary pulse shapes may in principle be built up by integrating a flux of the form (12); for example, rectangular pulses of length Δp give a result close to $(1 - \Delta p/p)\beta$. Observations of Her X1 make Δp about $p/3$, and so the pulse amplitude

$(f_{\max} - f_{\min})p/\int_0^p f(t)dt$ should be approximately 20%.

Figure 7 shows the shape of the reflected pulses when the X-ray pulsar has a knife beam pattern with $\Delta p = p/3$. One might imagine that, in this case (as well as in the case of the pencil beam pattern), an observer would see the pulsar beam running periodically along the stellar hemisphere from one edge to the other. However $A = R/cp \gg 1$, and so the observer will in fact see bright annuli moving away from some point on the stellar surface (when $\zeta = 0.5$, this point is near to the inner lagrangian point): this is rather similar to the situation considered above. This point is such that the light travel time from the source to the observer via it has a minimum value.

e) Short Time-Scale Optical Pulsations

The results obtained above for the pulsation of the reflected X-ray flux may be used to study the optical pulsation of HZ Her (Davidson *et al.*, 1972). It has already been noted (Basko and Sunyaev, 1973) that

emission lines are produced in a hot optically thin region: they should, therefore, respond quite quickly to short time-scale variations in the primary X-ray flux. The pulse amplitude of the line emission is probably about 10–20% which is close to that of the reflected X-rays; however, line emission is only a small fraction of the total optical flux, and so this amplitude is actually rather small (0.1 ÷ 0.2%). It is quite likely that much of the observed optical pulse amplitude is in fact due to emission lines, in spite of their low energy content, since a major fraction of the optical flux which is produced by the reprocessing of pulsed X-rays has a rather long “exit”-time ($t_d \gg 1.24$ s, Basko and Sunyaev, 1973).

Figure 7 shows the variation of the optical amplitude with phase.

The optical emission lines of bright objects, such as the companions of the X-ray sources Cyg X1, 2U1700–37 and 2U0900–40, should in principle have a short time-scale variability. Irregular “flickering” of the X-ray flux on a time scale $0.1 \text{ s} \leq p \leq 10 \text{ min}$ have been observed for these sources: emission lines (of He II, highly ionised heavy elements, and of the Balmer series) are produced when X-rays heat the region above the photosphere, and so changes in X-ray flux should induce corresponding changes in the line intensities.

Now, the intensity of a line depends rather critically on the temperature and density of the plasma, and so various kinds of behavior are possible. The thermal relaxation time in the optically thin region is small, and so to all intents and purposes the amplitude with which the line intensity varies depends on $A = R/cp$. The most favourable situation occurs when the characteristic period p of the X-ray variations is large ($\gg R/c$): in this case the line may vary with almost the same amplitude as the soft (0.5–10 keV) X-rays. In the case of Cyg X1, $p \sim 0.1$ s and $R \sim 10^{12}$ cm; the emission lines should then vary with an amplitude β of between 0.1% and 1%. Further optical lines should be produced through reprocessing of X-rays by gas in the binary system and in the outer parts of the disk formed by the matter accreting onto the compact object (Shakura and Sunyaev, 1973): these lines could contribute also to the optical variability of the system.

Observations of fast emission line variability may help to clarify the way in which X-rays are reprocessed in binary systems. Note that the atmosphere of the hot star owes much of its opacity to scattering on free electrons, and so a considerable amount of X-ray radiation is absorbed in a region which is actually transparent to optical radiation. Hence, a hot companion whose optical energy flux is very much greater than that of the X-ray source may exhibit quite significant optical fluctuations. Gnedin and Sunyaev (1973) have shown that one more source of pulsating optical radiation may exist in the X-ray binary system, namely the hot spots near the magnetic poles of a neutron star. At these spots the matter, accreting along the magnetic field lines, encoun-

ters the stellar surface. Just these spots are responsible for the X-ray emission (Pringle and Rees, 1972; Lamb *et al.*, 1973).

The ions of heavy elements (carbon, oxygen etc.) in the accreting flux have a huge kinetic energy $E_i \sim 2$ BeV, corresponding to 150 MeV per nucleon. At the surface, when being decelerated, these ions acquire a transversal with respect to the magnetic field velocity. Consequently, a powerful cyclotron emission of these ions arises at frequencies $\nu_i = \frac{Z_i e H}{2\pi m_i c} = \frac{Z_i}{A_i} \frac{e H}{2\pi m_p c}$. When the magnetic field H is of the order of 10^{12} Gauss and $Z_i/A_i \sim 1/2$, the gyrofrequencies of ions get into the optical region, but the gyrofrequency of electrons

$$\nu_e = \frac{m_p}{m_e} \frac{A_i}{Z_i} \nu_i \approx 2000 \frac{A_i}{Z_i} \nu_i$$

gets now into X-ray region²).

Consequently, the region emitting magnetobremstrahlung of heavy ions is transparent with respect to free-free absorption and Compton scattering, since in a strong magnetic field the cross-sections of these processes for an extraordinary wave are reduced by the factor $(\nu_i/\nu_e)^2 \ll 1$. The ratio of the ion charge Z_i to its mass number A_i is determined by the processes of charge exchange.

The brightness temperature of magnetobremstrahlung of fast heavy ions is determined by their kinetic energy:

it may reach the values $T_b \sim 10^{12} \text{ K} \sim \frac{1 \text{ BeV}}{k}$. The gyro-lines should have a considerable spectral width $\Delta\nu/\nu \sim \frac{1}{\sqrt{3}} \sqrt{\frac{E_i}{m_i c^2}} \sim \frac{1}{5}$. The absorption on the thermal ions is important at the very centre of the line $\Delta\nu/\nu \ll 1$. So the total emission in gyrolines of all heavy ions $L_{\text{opt}} \sim 2\pi a^2 \sum_i \pi k T_b \frac{\nu_i^2 \Delta\nu_i}{c^2} \sim 2\pi a^2 \pi 2k T_b \frac{1}{3} \frac{\nu_{\text{opt}}^3}{c^2} \sim 10^{32} \text{ erg/s}$ may give a contribution of about $10^{-4} \div 10^{-3}$ to the total optical luminosity of the system despite the fact, that an emitting hot spot has rather small size $a \sim 10^5 \text{ cm}$. This optical flux should emerge in the form of a beam similar to that in X-rays (Basko and Sunyaev, 1974).

Thus, in a binary system with an X-ray pulsar one could expect two sources of pulsating optical emission of comparable power: one of them connected with the neutron star and the other – with the optical counterpart. The frequency of the optical pulsations of the first source should precisely coincide with that of X-ray pulses, while the optical radiation of the normal star should pulsate on the Doppler-shifted frequency of X-ray pulsations (this Doppler shift is due to the orbital

²) Naturally, in some models of X-ray sources, the existence of a powerful and narrow X-ray line, which corresponds to the cyclotron resonance $\nu_e = eH/2\pi m_e c$, is predicted (Gnedin and Sunyaev, 1973; Basko and Sunyaev, 1974).

motion of the normal component), and this effect has been already observed (Middleditch and Nelson, 1973).

V. X-ray Reflection and Reprocessing in Specific Systems

A) The HZ Her = Her X1 System

The values of plane albedo presented in Table 1 show that the surface area of the normal component reflects less than 30 ÷ 40% of the X-ray flux which falls on it. The remaining 60 ÷ 70% is used to heat the photosphere and emerges as optical and ultraviolet radiation with a blackbody spectrum. Consequently, the surface of the optical companion has a bright hot spot whose effective temperature T_{eff} is given by $T_0 \sqrt[4]{1 + \beta_x F_x/F_0}$, where T_0 is the effective temperature of that part of the star which is not exposed to the X-rays, F_0 is its own energy flux, and $\beta_x \approx 0.6$ is the fraction of energy absorbed. The present work confirms earlier calculations (Basko and Sunyaev, 1973) that the observed X-ray energy flux from Her X1 is quite enough to induce the observed optical variability of HZ Her. Since $F_x \gg F_0$ the maximum temperature of the photosphere can be calculated to be:

$$T_{\text{eff}} = \sqrt[4]{\beta_x F_x/b} = \sqrt[4]{\beta_x L_x/4\pi b A_1^2},$$

where b is the Stefan-Boltzmann constant.

Substituting now an X-ray luminosity L_x of 10^{37} erg/s , and a distance A_1 from the X-ray source to the inner lagrangian point of $2.5 \times 10^{11} \text{ cm}$ (Basko and Sunyaev, 1973), the value of this temperature turns out to be $\sim 2 \times 10^4 \text{ K}$, which may actually be greater than the observed value.

a) The 36-Day Periodicity of Her X1

The mechanism responsible for the 36 day period of Her X1 is not yet understood: X-rays are observed for only 12 days of the 36. At the same time, however, the optical variability of HZ Her (whose orbital period P is 1^d.7) due to the reprocessing of X-rays in the atmosphere of the normal companion is observed for all 36 days without break (Wenzel and Hessner, 1972). There appear to be two alternative interpretations: 1) the X-ray source precesses with a 36-day period (Brecher, 1972; Shklovsky, 1973; Novikov, 1973), but illuminates the Earth for just 12; the normal star, however, subtends a huge solid angle of ~ 0.6 ster at the X-ray source and so is illuminated to some extent for all 36 days;

2) the hard X-ray ($h\nu > 2 \text{ keV}$) source periodically turns off (Tananbaum *et al.*, 1972; Bisnovatyi-Kogan and Komberg, 1973); however, a hypothetical source of soft X-rays ($h\nu < 1 \text{ keV}$) does not, but continues to heat the hot spot on the surface of HZ Her and is therefore

responsible for its 1.7 day optical variability (Avni *et al.*, 1973; Pringle, 1973).

It might be possible to distinguish between these alternatives by observation of the hard ($h\nu \sim 15-30$ keV) X-rays.

In case (1), a reflected signal would be detected during the 24 day “quiet” period: its amplitude would be about 10% of the maximum, its spectrum should be harder than that of the primary flux, and its intensity should vary with a 1.7 day period (Fig. 1). Reflected pulses with a 1.24 s period should be suppressed, since their amplitude is $\sim 10-20\%$ of the average level.

In case (2), neither hard X-rays, nor the softer radiation at $h\nu \sim 2-6$ keV will be observed at all for 24 days.

Note that it is not entirely unfeasible to detect the reflected signal against the background of the primary flux. On the one hand, the reflected pulse has considerable linear polarisation whose degree varies with the orbital phase. On the other, the amplitude of the reflected pulse is small, and so it may be detectable between the pulses of the primary one. Finally, high resolution spectra may show up the K_α -line of iron.

b) The Possible Existence of a Soft X-ray Source

Case (2) in the previous subsection requires that there be a source of soft X-rays with $h\nu < 1$ keV in the HZ Her system. We now show below that this is most unlikely, since its optical characteristics cannot be generated by the reprocessing of soft X-rays in the atmosphere of the normal star.

UBV and spectral observations (Lyutiy *et al.*, 1973; Davidsen *et al.*, 1972; Crampton and Hutchings, 1972) show that the surface temperature of the region facing the X-ray source decreases rapidly with distance from the point closest to the source. Absorption lines corresponding to spectral types B2 \div A7 are observed (Crampton and Hutchings, 1972): this suggests that the optical radiation passes through layers which are cooler than the radiation itself. Therefore, it follows that the X-rays which were transformed into optical radiation must have penetrated the stellar atmosphere to a considerable depth. It has been shown (Basko and Sunyaev, 1973) that the reprocessing of hard X-rays of Her X1 can account for the observed characteristics of HZ Her. Can a source of soft X-rays having the same power act in the same way?

The spectral types of HZ Her in different phases determined by *UBV* measurements (Lyutiy *et al.*, 1973) are the same as those found by spectrometry (Davidsen *et al.*, 1972; Crampton and Hutchings, 1972). They suggest that the photosphere of the star is close to thermodynamic equilibrium. Therefore, the temperature T_e of the region where the optical spectrum is formed cannot be much greater than 1.6×10^4 K, which corresponds to the earliest observed spectral type B2. At such a low temperature, X-ray photons with $h\nu$

between 55 eV and 1 keV have a large photoabsorption cross-section (these photons are to a large extent absorbed by the ions He I and He II as well as by carbon and oxygen).

Let us now assume that the atmosphere of HZ Her has an exponential density distribution. Then:

$$N_e = N_{e0} \exp(-z/H),$$

where

$$H = kT_e R^2 / m_p G M.$$

Putting

$$M = 1.7 M_\odot$$

$$R = 2.5 \times 10^{11} \text{ cm},$$

we find that $H = 2.3 \times 10^4 T_e \text{ cm} = 4 \times 10^8 \text{ cm}$.

Now free-free absorption makes the main contribution to the opacity at $T_e \sim 1.6 \times 10^4$ K and the optical depth is given by:

$$\tau_{\text{ff}} = \int_0^\infty \kappa_{\text{ff}} dz = 6.5 \times 10^{-24} N_{e0}^2 T_e^{-7/2} H/2 = 1. \quad (13)$$

The optical depth of this layer with respect to photoabsorption even for photons of $h\nu = 1$ keV is 80, while for photons with $h\nu = 250$ eV and 50 eV it is 2.6×10^3 and 3×10^5 respectively. The free-free absorption coefficient κ_{ff} has been taken to be $6.5 \times 10^{-24} N_e^2 T_e^{-3.5} \text{ cm}^{-1}$ (Zeldovich and Raizer, 1966). The density N_e in the layer where the spectrum is formed may be estimated from (13), and turns out to be $\sim 7 \times 10^{14} \text{ cm}^{-3}$. At such a high density and low temperature, the ionization of helium and the heavy elements does not prevent X-rays being absorbed because the recombination rate is high. Thus, soft X-rays are absorbed in a region which is transparent to optical radiation, and so cannot give rise to a blackbody spectrum. We recall that the optical depth with respect to photoabsorption becomes equal to that for free-free absorption when X-rays have an energy of ~ 4 keV (in this particular model), whereas the energy of the observed X-ray spectrum of HZ Her is mainly at $h\nu \sim 20 \div 30$ keV.

We might also suppose that the observed optical flux is emitted by a hot region above the surface which is thin with respect to absorption of optical quanta (Arons, 1973). This is rather unlikely to be the case here, since there would then be no way to form the absorption lines. Moreover, a hot optically thin plasma normally radiates only a small fraction of its energy in the optical continuum, but dissipates much of its energy in emission lines: these simply are not observed.

B) X-ray Pulsars, Whose Beams do Not Scan the Earth

The results obtained in this paper lead us to suggest that there should exist X-ray sources which are weak in the spectral range $\sim 2 \div 6$ keV and are bright at $\sim 15 \div 20$ keV. These sources should vary in a sinusoidal

way and have the typical periods of close binary systems.

Consider a close binary system, of which one member is a compact object (possibly a neutron star) and is a source of tightly beamed X-rays, and of which the other is a normal star which fills its Roche lobe. Let us suppose further that the beam never strikes the Earth: nevertheless, the normal star subtends a sufficiently large angle at the X-ray source ($\sim 0.5 \div 1$ ster), and we shall assume that some part of its surface is always illuminated by the beam. This is by no means an unlikely situation: the X-ray pulsars Her X1 and Cen X3 are members of close binary systems and have beams which are sufficiently narrow for there to be points in space from which they will not be visible.

a) The Spectrum of the Reflected X-rays

When the primary spectrum takes the form $F_x(\nu) \propto \exp(-h\nu/kT_x)$ with $kT_x \sim 15 \div 40$ keV, the spectrum of the reflected X-rays takes the Wien form with a maximum intensity at $h\nu \sim 15 \div 20$ keV. Fine structure due to K-jumps; K_α -emission of iron, sulphur and so on (see Fig. 2; IV, a) may be present.

b) Variability

The X-ray flux reflected by the normal star may be detectable on the Earth. Since the binary system rotates the reflected signal will fluctuate with the period of the system, and its amplitude will depend strongly on the inclination of the orbit i . The top of Fig. 1a shows the light curves of a binary system in reflected X-rays for $i = 90^\circ$, 15° and 0° (the straight line). These curves are not sensitive to changes in the parameters of the binary system when the normal star more or less fills its critical Roche lobe. For comparison, the light curve in primary X-rays for $i = 90^\circ$ is also shown.

In the case, when the X-ray luminosity of the pulsar greatly exceeds the own luminosity of the optical component of the binary system, the optical luminosity of the system may be mainly due to the X-ray reprocessing by the atmosphere of the normal star. This is similar to the case of HZ Her. Both, the reflected X-ray flux and the optical emission of the area of the normal star heated by X-rays, may be observed now. In this situation the maxima and minima of the X-ray light curve should coincide in orbital phase with maxima and minima of the optical and infra-red light curves.

c) The Source Cyg X3

The curve in Fig. 1a corresponding to $i = 15^\circ$ resembles the X-ray light curve of the source Cyg X3 (Parsignault *et al.*, 1972) which has had no firm theoretical interpretation up to now. It is possible that this source is a close binary system of just the type discussed above. The flat spectrum in the range $h\nu \sim 3 \div 6$ keV may be due to the presence of a highly ionized diffusive layer

with $\tau_0 \gtrsim 0.3$ (see IV, b). The reflected X-ray flux should be linearly polarized in all phases because the orbital inclination is small. Short time-scale fluctuations in the primary flux may be considerably damped out after reflection. If the observed flux is mainly reflected by a hot diffusive layer whose depth $l \sim cp$ is large, then rapid variations are damped out both by the mechanism discussed in Section IV, d and because the light takes a finite time to cross this zone. In fact Cyg X3 has not been seen to pulsate, at least not in the time range between 0.1 s and 1 s (Parsignault *et al.*, 1972).

A 21 cm absorption measurements for the radioflare observed within the position error box of Cyg X3 (Lauque *et al.*, 1972) give the distance of the radiosource $\gtrsim 11$ kpc. If in fact the radio- and X-ray source are one and the same object then it is easy to estimate the observed X-ray luminosity L_x to be $\sim 3 \times 10^{38}$ erg s $^{-1}$ (we have assumed that the X-ray temperature is 30 keV). If we really detect only the X-rays reflected by the normal star, and if the inclination of the orbit is $\sim 15^\circ$, then the X-ray luminosity of the primary source should be ~ 25 times more, namely $L_x \approx 7 \times 10^{39}$ erg s $^{-1}$.

This value strongly exceeds the Eddington limit $L_e \approx 10^{38} \left(\frac{M}{M_\odot} \right)$ erg s $^{-1}$, which is likely to be an upper

limit for the X-ray luminosity of the accreting neutron star (the neutron star is assumed to account for the pulsar effect). Thus, the assumption of accreting neutron star as an X-ray source in Cyg X3 system meets severe difficulties.

These difficulties disappear, however, if only one assumes that the X-ray pulsar in Cyg X3 system is a non-accreting young one (similar to that in Crab Nebula) with a very short period $p \lesssim 0.01$ s and, respectively, with a supercritical luminosity. The system Cyg X3 has many peculiar features and, most likely, a short evolutionary time-scale. The supernova explosion in it could have occurred not long (~ 100 years) ago and been unobserved due to a large distance and strong interstellar absorption. In this model the radioflares of Cyg X3 can be easily explained as emission of a cloud of relativistic electrons ejected by the pulsar starquake. Because of the large free-free optical depth and high plasma frequency, the stellar wind evaporated from the surface of the normal star absorbs the radioemission of the pulsar itself to an unobservable level. The powerful infra-red beam of the young pulsar does not scan the Earth. But its reflection from the diffusive layer (similar to that of X-rays) may account for the observed infra-red variability of Cyg X3 (Becklin *et al.*, 1973).

d) The Source 2U 1700-37

A comparatively smooth X-ray light curve of the source 2U 1700-37 (Jones *et al.*, 1973) suggests that this object can be interpreted in a similar way with an

inclination $i \sim 90^\circ$ (Cherepashchuk and Sunyaev, 1973). If this is in fact a binary visible only in reflected X-rays then we will be able to explain in a coherent way (among other features): a remarkably long eclipse duration ($\sim 120^\circ$), a low X-ray luminosity: $L_x \sim 1 \div 3 \times 10^{36}$ erg/s, the behaviour of the amplitude of the intensity variations of different time-scales, a rather variable cut off (which would be due to a variable optical depth of the diffusive layer). A secondary minimum at phase $\zeta = 0.5$ may be interpreted as due to occultation by a disk made up of matter accreting onto the neutron star.

The results obtained in subsection IV, d show that the reflected X-ray flux should fluctuate with the pulsar period p (which is unknown now) and amplitude of the order $\sim 5\% \times (p/1\text{ s})$. The decrease in the amplitude compared to HZ Her = Her X1 system is due to the larger size of the visible star $R_v \sim 10^{12}$ cm. It is interesting also to try to find out the weak optical fluctuations on the pulsar frequency due to the X-ray reprocessing by the atmosphere of the bright optical star.

Acknowledgement. The authors wish to thank Ya.B.Zeldovich, I.L.Beigman, A.M.Cherepashchuk and A.M.Urnov for valuable discussions.

References

- Achiezer, A.I., Berestetski, V.B. 1969, Quantum Electrodynamics, Nauka, Moscow
- Arons, J. 1973, *Astrophys. J.* **184**, 539
- Avni, Y., Bahcall, J.N., Joss, P.C., Bahcall, N.A., Lamb, F.K., Pethick, C.J., Pines, D. 1973, *Nature Phys. Sci.* **246**, 36
- Bahcall, J.N., Bahcall, N.A. 1972, *Astrophys. J.* **178**, L1
- Basko, M.M., Sunyaev, R.A. 1973, *Astrophys. Space Sci.* **23**, 117
- Basko, M.M., Sunyaev, R.A. 1974, (submitted to *Astron. & Astrophys.*), preprint
- Becklin, E.E., Neugebauer, G., Hawkins, F.J., Mason, K.O., Sanford, P.W., Matthews, K., Wynn-Williams, C.G. 1973, *Nature* **245**, 302
- Bell, K.L., Kingston, A.E. 1967, *Monthly Notices Roy. Astron. Soc.* **136**, 241
- Bethe, H.A., Salpeter, E.E. 1957, Quantum Mechanics of One- and Two-Electron Atoms, Acad. Press, New York
- Bisnovatyi-Kogan, G.S., Komberg, B.V. 1973, *Astron. Zhirk.*, No. 784
- Brecher, K. 1972, *Nature* **239**, 325
- Brown, R.L., Gould, R.J. 1970, *Phys. Rev. D* **1**, 2252
- Cherepashchuk, A.M., Sunyaev, R.A. 1973, *Monthly Notices Roy. Astron. Soc.* (in press)
- Crampton, D., Hutchings, J.B. 1972, *Astrophys. J.* **178**, L65
- Davidson, A., Henry, J.P., Middleditch, J., Smith, M.E. 1972, *Astrophys. J.* **177**, L97
- Fink, R.W., Jopson, R.C., Hans Mark, Swift, C.D. 1966, *Rev. Mod. Phys.* **38**, 513
- Forman, W., Jones, C.A., Liller, W. 1972, *Astrophys. J.* **177**, L103
- Gnedin, Yu.N., Sunyaev, R.A. 1974, *Astron. & Astrophys.* (in press)
- Gursky, H. 1972, preprint "Galactic X-Ray Sources", Lectures at the summer School on Black Holes, Les Houches, France
- Ivanov, V.V. 1969, Radiative Transfer and Celestial Body Spectra, Nauka, Moscow
- Jones, C., Forman, W., Tananbaum, H., Schreier, E., Gursky, H., Kellogg, E., Giacconi, R. 1973, *Astrophys. J.* **181**, L43
- Lamb, F.K., Pethick, C.J., Pines, D. 1973, *Astrophys. J.* **184**, 271
- Lauque, R., Lequeux, J., Nguyen-Quang-Rieu 1972, *Nature* **239**, 119
- Lyutiy, V.M., Sunyaev, R.A., Cherepashchuk, A.M. 1973, *Astron. Zh.* **50**, 3
- Middleditch, J., Nelson, J. 1973, *Astrophys. Letters* **14**, 129
- Novikov, I.D. 1973, preprint, *Astron. Zh.* **50**, 459
- Parsignault, D.R., Gursky, H., Kellogg, E.M., Matilsky, T., Murray, S., Schreier, E., Tananbaum, H., Giacconi, R., Brinkman, A.C. 1972, *Nature* **239**, 123
- Pringle, J.E. 1973, *Nature Phys. Sci.* **243**, 90
- Pringle, J.E., Rees, M.J. 1972, *Astron. & Astrophys.* **21**, 1
- Shakura, N.I., Sunyaev, R.A. 1973, *Astron. & Astrophys.* **24**, 337
- Shklovsky, I.S. 1967, *Astron. Zh.* **44**, 930
- Shklovsky, I.S. 1973, *Astron. Zh.* **50**, 233
- Sobolev, V.V. 1972, Light Scattering in the Planet Atmospheres, Nauka, Moscow
- Tananbaum, H. 1972, Proceedings of IAU Symposium No. 55, Ed. R. Giacconi and H. Bradt, Reidel, Dordrecht
- Tananbaum, H., Gursky, H., Kellogg, E.M., Levinson, R., Schreier, E., Giacconi, R. 1972, *Astrophys. J.* **174**, L143
- Ulmer, M.P., Baity, W.A., Wheaton, W.A., Peterson, L.E. 1972, *Astrophys. J.* **178**, L61
- Wenzel, W., Hessner, M. 1972, IBVS, No. 733
- Zeldovich, Ya.B., Raizer, Yu.P. 1966, Physics of Shock Waves and High-Temperature Hydrodynamic Phenomena, Nauka, Moscow
- M. M. Basko
R. A. Sunyaev
Institute of Applied Mathematics Academy
of Sciences of the USSR,
Miusskaja pl. 4, Moscow 125047, USSR
- L. G. Titarchuk
Institute for Cosmic Research Academy
of Sciences of the USSR
Profsoyusnaja, 88, Moscow 117485, USSR